

Next-Scale Autoregressive Models are Zero-Shot Single-Image Object View Synthesizers

Shiran Yuan
UC Berkeley

shiran.yuan@berkeley.edu

Hao Zhao
Tsinghua University

zhaohao@air.tsinghua.edu.cn

Abstract

Methods based on diffusion backbones have recently revolutionized novel view synthesis (NVS). However, those models require pretrained 2D diffusion checkpoints (e.g., Stable Diffusion) as the basis for geometrical priors. Since such checkpoints require exorbitant amounts of data and compute to train, this greatly limits the scalability of diffusion-based NVS models. We present Next-Scale Autoregression Conditioned by View (ArchonView), a method that significantly exceeds state-of-the-art methods despite being trained from scratch with 3D rendering data only and no 2D pretraining. We achieve this by incorporating both global (pose-augmented semantics) and local (multi-scale hierarchical encodings) conditioning into a backbone based on the next-scale autoregression paradigm. Our model also exhibits robust performance even for difficult camera poses where previous methods fail, and is several times faster in inference speed compared to diffusion. We experimentally verify that performance scales with model and dataset size, and conduct extensive demonstration of our method’s synthesis quality across several tasks. Our code is open-sourced at <https://github.com/Shiran-Yuan/ArchonView>.

1. Introduction

Humans, living in a 3D world, naturally infer the complete 3D structure of objects from a single 2D view, leveraging prior knowledge and spatial reasoning. If machines could achieve the same, particularly in a zero-shot manner for unseen objects, it would greatly benefit fields such as 3D content creation, simulation, and real-world perception systems. Consequently, zero-shot novel view synthesis (NVS) from single object-centric images emerges as a fundamental challenge in computer vision. Since this is a highly under-constrained problem, it is typically formulated as a generative task conditioned on the input image and relative camera pose. The prevailing approach fine-tunes a 2D diffu-

sion model to exploit implicit geometric priors learned from large-scale image datasets. Whilst this paradigm has shown promising results, it comes with several limitations.

The primary limitation of diffusion-based NVS models lies in their reliance on pretrained 2D diffusion backbones, which require vast amounts of data and computational resources—far beyond what is accessible to most researchers. This fundamental constraint makes scaling diffusion-based NVS models extremely challenging. Notably, to the best of our knowledge, no prior work has demonstrated scaling trends with respect to model size for single-image object-centric NVS. Another critical limitation of diffusion models is their inherent trade-off between speed and quality. Due to the need for multiple denoising steps through a U-Net structure, achieving high-quality outputs inevitably results in relatively slow inference. Consequently, even if diffusion models were scalable, larger models would further increase inference time and computational cost, potentially rendering them impractical for real-world deployment.

Such downsides of diffusion call for a paradigm shift: a backbone which can be readily scaled up, does not require 2D pretraining, is more efficient, and outputs better results. To this end we propose Autoregression Conditioned by View (ArchonView), the first NVS model based on visual autoregressive generation. We base our method on the recently proposed next-scale autoregression backbone, which replaces raster-scan-ordered next-token prediction in conventional visual autoregression with autoregressively predicting the next resolution scale of tokens in a coarse-to-fine manner (described in Sec. 3.2). Whilst previous works have verified its scalability and applicability to many tasks in vision, so far, its applicability to NVS remains unknown.

In order to adapt autoregression to NVS, we condition the model in two ways: globally, through a posed CLIP encoding, which allows the model to gain semantic information augmented by the desired relative pose (described in Sec. 3.3); and locally, encoded by the multiscale VQ-VAE representation (which is also used for quantization in the main generative architecture), enforcing consistency in

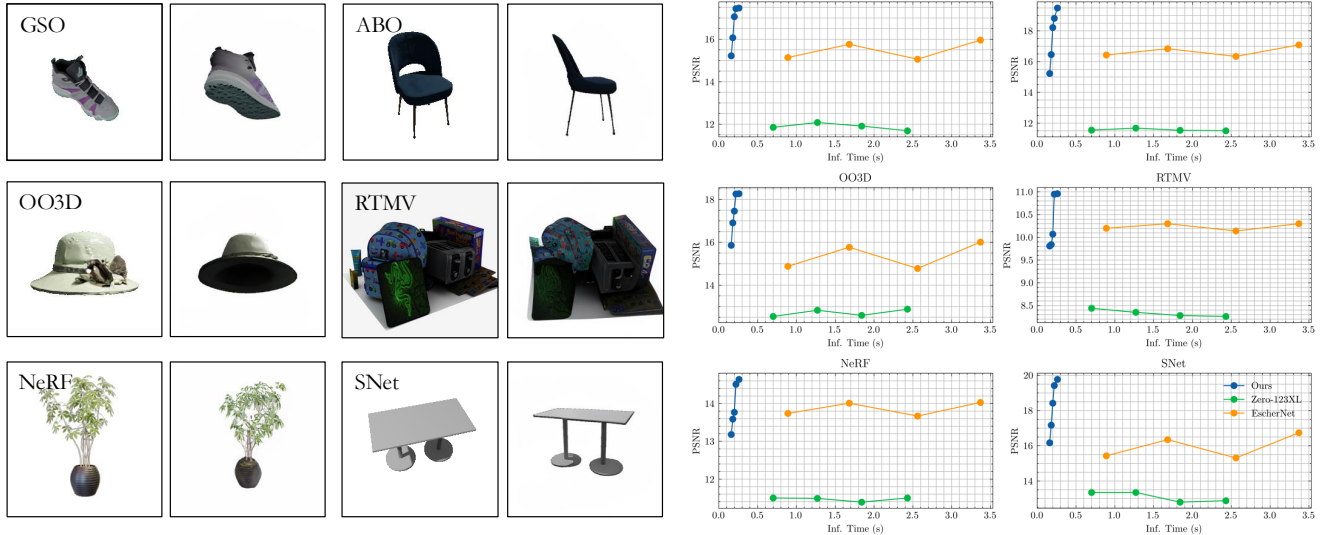


Figure 1. **Fast, accurate, and scalable novel view synthesis without 2D pretraining.** Displayed on the left are results sampled from each of our test datasets, where the left image shows the input and the right image is a novel view from our model. Note that all of the displayed results are from zero-shot inference. On the right are time *v.s.* PSNR tradeoff plots, where our models scaled to different parameter sizes are compared against diffusion models with different denoising steps.

local details with the input image (described in Sec. 3.4). Experimentation shows that our method achieves state-of-the-art performance consistently and robustly across multiple benchmarks, scales with both model size and dataset size, and is several times faster than current diffusion-based methods. Some of our results across different evaluation datasets and comparisons with current methods are shown in Fig. 1.

In summary, our key technical contributions to the field of zero-shot single-image NVS are as follows:

- We present a method that does not require any pretraining on 2D data, thereby drastically lowering the computation and data requirement for training a model from scratch.
- Our method consistently achieves state-of-the-art performance and is also several times faster in terms of inference time compared to previous works.
- We demonstrate that our method scales with both model size and dataset size.
- We are the first to base a model on an autoregressive backbone for this task, demonstrating the potentials of next-scale autoregression.

2. Related Works

2.1. Generative Modeling

Autoregression has seen many applications to generation of language [5, 59, 60, 77], world models [6, 43, 79], videos [34, 85, 89], and multimodal outputs [7, 32, 53, 74]. Besides being efficient and accurate enough for operational use, it has also been shown to be scalable in

many tasks [27, 31]. However, the current predominant paradigm of 2D generative modeling is indubitably diffusion, thanks to multiple groundbreaking innovations in this field [28, 56, 67, 96]. Meanwhile, though conventional visual autoregression (using a raster-scan traversal of fixed-size patches as tokens) has produced innovative techniques [21, 38, 54, 80, 94] and achieved some milestones [14, 62, 63, 95], advances in diffusion left it largely irrelevant.

Recently, the newly proposed next-scale prediction paradigm of autoregression [76], replacing the conventional raster-scan next-token paradigm, has been proven effective, developed upon [25, 64, 65, 75], and adapted [26, 39, 44, 90, 97]. Empirical evidence demonstrates its reliability in achieving accurate, efficient, and scalable results, exceeding diffusion models in many tasks where raster-scan autoregression struggles. This has reignited interest in using autoregressive models for visual generative tasks where diffusion models currently dominate.

2.2. Novel View Synthesis

Before the advent of generative NVS models, predominant methodologies have used implicit representations [1–3, 47], voxel-like representations [13, 22, 73, 92], explicit primitives [29, 33, 45, 48], *etc.* to model 3D scenes or objects based on given views and poses, thus achieving NVS. However, in the case of sparse inputs, where few views or only one view is available, none of those models are able to produce accurate results due to the scene being severely under-constrained.

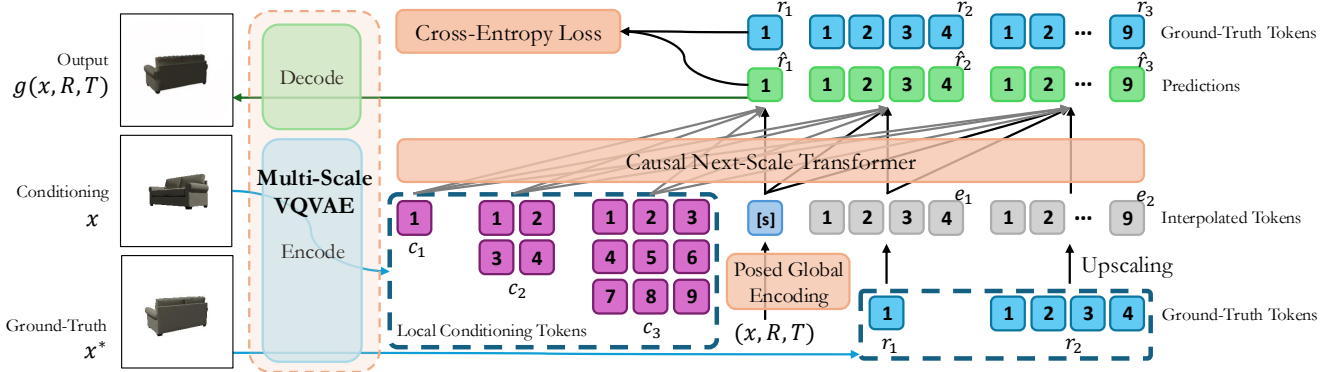


Figure 2. **The overall architecture for the training of ArchonView.** The predictions are classifier logit predictions, and can be converted to images after sampling based on the logit probabilities. The loss calculation is directly based on the logits and does not involve sampling.

While some efforts have been made to adapt conventional frameworks to sparse-input scenarios [12, 15, 30, 51, 88, 93], their capabilities were limited, or often depended on strict hypotheses regarding geometrical priors. In addition, most aforementioned methods require specific training or fine-tuning on the scene or object in question, or were fine-tuned on a class of objects (*e.g.*, from ShapeNet [11]) and only perform well for in-distribution inputs. Thus, none achieved capability for zero-shot single-image NVS with such paradigms.

2.3. Generative NVS

Early works have used GANs [24] as backbones for conducting NVS generatively, reframing the problem as modeling the distribution of scene views conditioned by camera pose [8, 9, 23, 49, 50, 71]. In late 2022 through 2023 there was a surge of works using diffusion models for NVS, often coupled with the then-recent NVS representations (*e.g.* NeRF); in particular, some works used diffusion models as priors for supervising the training of a 3D representation model [4, 19, 46, 69, 82, 86], while others directly used diffusion models with camera pose conditioning as an NVS representation backbone [10, 40, 83] (interestingly the latter’s methodology of view generation based on latents coincides with previous works using transformers [36, 66, 68]).

A particularly important work in this period was Zero 1-to-3 [40], which was fine-tuned on an image variation model [57] which, in turn, was tuned on Stable Diffusion [67]. Its main conclusion was that 2D diffusion models already contain 3D-aware priors, and that such priors can be directly extracted by fine-tuning pretrained 2D diffusion checkpoints. This paradigm of fine-tuning 2D diffusion models for priors spawned a line of works [35, 41, 72, 84, 91, 98] which similarly attempt to extract 3D-aware priors from pretrained 2D diffusion models. In our work, we demonstrate that autoregressive models can directly have such 3D-awareness without 2D pretraining.

3. Methodology

3.1. Motivation

Problem Formulation Formally, we wish to solve the following problem. Given a single input view x of an underlying 3D object, as well as relative camera transformations $R \in \mathbb{R}^{3 \times 3}$ and $T \in \mathbb{R}^3$, we would like to create a probabilistic model $g(x, R, T)$ such that the output view

$$x_{R,T}^* \sim g(x, R, T) \quad (1)$$

follows the distribution of the transformed view from applying the relative camera transformation (R, T) on x .

Diffusion is Not All You Need The current predominant formulation of our problem is as a diffusion model. Specifically, common architectures based on the latent diffusion paradigm [67] are made up of an image encoder-decoder pair $(\mathcal{E}, \mathcal{D})$, a U-Net denoiser ϵ_θ , and a conditioning encoder τ . The latents $z \sim \mathcal{E}(x)$ are then corrupted with additive Gaussian noise at each step, forming noised latents z_t . Diffusion models are thus trained based on the objective

$$\min_{\theta} \mathbb{E}_{z \sim \mathcal{E}(x), \epsilon \sim \mathcal{N}(0,1), t} \|\epsilon - \epsilon_\theta(z_t, t, \tau(x, R, T))\|_2^2. \quad (2)$$

However, we notice a key downside of this formulation; zero-shot capabilities in this line of research are dependent upon priors within 2D pretrained diffusion models. For instance, one can compare [83] with [40], which are both based on the presented model; the former was not tuned from 2D models and thus did not exhibit zero-shot abilities, while the latter was tuned from Stable Diffusion and used CLIP for conditioning encoding, thus allowing zero-shot NVS. This naturally leads to a scalability issue: since the underlying checkpoints require large amounts of data and computation to train, it is difficult to scale existing models up. To the best of our knowledge, most or potentially all works in this direction are tuned from Stable Diffusion. Diffusion models also have other problems such as relatively

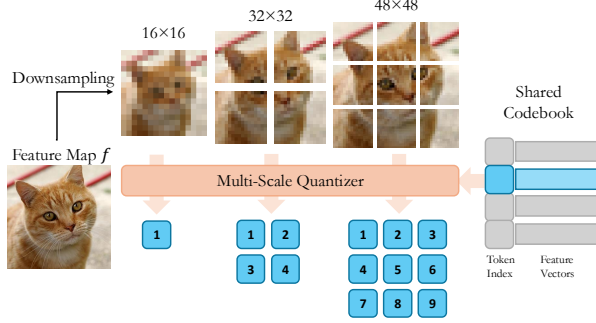


Figure 3. **Structure of the multi-scale VQVAE.** The VQVAE operates by converting the input image into a feature map, resizing the feature map into different scales, and using a codebook shared between scales to compress the patch tokens. Note here f is aesthetically represented as an image whereas it is actually an encoded version of the image.

slow inference speed (due to repeated denoising passes), which further limit their effectiveness.

3.2. Backbone Architecture

We propose using next-scale autoregression [76] as our backbone paradigm instead and modifying it to suit our task. Our overall architecture during training is shown in Fig. 2. Next-scale autoregression is based on predicting the next resolution scale of the image in a coarse-to-fine manner, and consists of two main parts: a multi-scale vector-quantized variational autoencoder (VQVAE) [80] which supports image tokenization (depicted in Fig. 3), and a transformer which autoregressively predicts the next scale of tokens (depicted in Fig. 4).

Multi-Scale Tokenization The VQVAE contains an image encoder-decoder pair (\mathcal{E}, \mathcal{D}), a quantizer \mathcal{Q} , and a learnable codebook Z with vocabulary size V . The image encoder takes an image x as input and encodes it into a feature map $f = \mathcal{E}(x) \in \mathbb{R}^{h \times w \times C}$ (where h, w are the latent height/width, and C is the embedding dimension). Note that the latent dimensions of the image are based on patching, similar to conventional autoregression and latent diffusion. The feature maps are then quantized as $q = \mathcal{Q}(f) \in [1..V]^{h \times w}$. The quantizer does this by mapping each patch $f_{i,j}$ to the Euclidean nearest codebook entry Z_v :

$$q_{i,j} = \arg \min_{v \in [1..V]} \|Z_v - f_{i,j}\|_2. \quad (3)$$

The key to the multi-scale formulation is that the input image is resized into different resolution scales. For instance, since we use 16×16 patches, the 3×3 scale would reshape the image to 48×48 pixel resolution before tokenization; and the corresponding scale token would contain 9 patch tokens. All scales share the same codebook Z , thus ensuring a consistent vocabulary is used across different token scales.

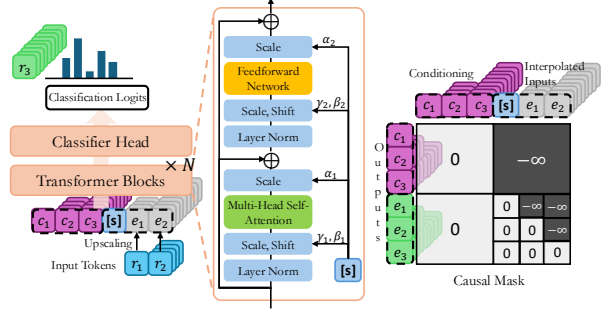


Figure 4. **The next-scale prediction transformer architecture.** Next-scale prediction operates by passing local conditioning tokens and input tokens through multiple transformer blocks which are conditioned by adaptive layer normalization. The transformers use an attention bias mask to enforce the autoregressive causality constraint.

The image can then be reconstructed using the decoder \mathcal{D} given the quantized tokens.

Next-Scale Prediction Transformers Based on a frozen VQVAE (trained on a compound loss as in [76]), the autoregressive model is formulated as follows. We attempt to achieve a probabilistic model p_θ (the next-scale transformer) conditioned by our inputs (x, R, T) such that the joint likelihood of scale tokens (r_1, r_2, \dots, r_K) representing the distribution of $x_{R,T}^*$ can be modeled as

$$g(x, R, T) = p_\theta(r_1, r_2, \dots, r_K | x, R, T) \quad (4)$$

$$= \prod_{k=1}^K p_\theta(r_k | x, R, T, r_1, r_2, \dots, r_{k-1}).$$

Note that here the autoregressive assumption is that each scale r_k only depends on the conditioning and the previous scales (similar to a coarse-to-fine process), instead of the later scales. We add conditioning tokens c_k (details in Sec. 3.4) as well for additional information, and the causal mask used for transformers is as displayed in Fig. 4.

We use teacher forcing to train the model, where $(r_1, r_2, \dots, r_{K-1})$ of x^* and conditioning from x are used for causally predicting all tokens (r_1, r_2, \dots, r_K) of x^* . After sending inputs and conditioning through several transformer blocks, the eventual results are passed through a classifier head (consisting of a single linear layer) and outputted as classification logits, after which the cross-entropy loss between the logits and ground truths is taken for back-propagation.

Implementation-wise, each scale token r_k is first interpolated to the same size as r_{k+1} by taking the corresponding feature map f , resizing it accordingly, and applying tokenization. An exception is the $[s] \rightarrow r_1$ mapping, which does not require resizing. The upscaled results e_k are

then taken as input to the causal transformer. Each attention layer uses adaptive layer normalization (AdaLN) [56] conditioned by the start token (to ensure consistency with the global encoding conditioning) and multi-head self-attention [81]. We refer to the number of AdaLN transformer blocks per prediction step as the model depth and the dimension of tokens C as the model width. For easy scaling, in our experiments we set the model width to always be 64 times the depth.

During inference, we first find c_k and the start token [s] using x . We then use them to infer the distribution of r_1 and sample from the distribution. We then use the available information to infer r_2 , and so on. Note that already known tokens are kv-cached [58] and not replaced in further inference steps. The final inferred r_k values are passed through the VQVAE decoder to arrive at \hat{x}^* .

The Devil is in the Classifier Head The original formulation of the next-scale transformer [76] applies adaptive normalization before the classifier head as well. However, as we will demonstrate in experiments, in our task this restricts the performance of the resulting model considerably. We theorize that this implies global conditioning using AdaLN must be accompanied by self-attention with local conditioning tokens (as the classification logit prediction step does not involve attention transformers), and that otherwise only using global conditioning would prompt the output image to “forget” details from local conditioning. After the removal of this normalization step, our results improved considerably.

3.3. Semantic Global Pose Conditioning

We now start presenting the details of how we adapted the architecture via adding conditioning for our task. Firstly, we need to choose a start token that reliably captures global information from our conditioning (x, R, T) , because it will be used both for initializing the autoregressive procedure and for normalization of every attention layer, which means it should have complete field of view. Meanwhile, it must also be a single token because it will be mapped to the first resolution scale (which comprises of a single patch) during autoregressive inference.

To balance those two needs, we would like an encoding scheme that could condense semantic information from the image along with the query poses into a vector of size comparable to tokens. Inspired by [40], we use a “Posed CLIP” embedding as follows:

$$\tau(x, R, T) = W(W_i(\text{CLIP}(x) \oplus [\theta, \sin \phi, \cos \phi, r]) + b_i) + b. \quad (5)$$

Here, θ , ϕ , and r respectively stand for the relative elevation, azimuth, and radial distance of the transformation; \oplus stands for concatenation along the feature dimension; $\text{CLIP}(x) \in \mathbb{R}^{768}$ is the CLIP visual embedding [61],

which we use here as a global semantic encoder; and (W_i, b_i) , (W, b) are two pairs of linear layer parameters, where the i subscript stands for identity initialization (*i.e.* W_i is initialized as a generalized identity matrix and b_i is initialized as a zero vector).

We add classifier-free guidance by randomly replacing values in the 768-dimensional posed CLIP embedding (which has gone through (W_i, b_i) but not (W, b) yet) with values from a null CLIP text embedding (applying the CLIP text encoder to an empty string).

The two linear layers here serve different purposes. The identity-initialized layer $W_i \in \mathbb{R}^{768 \times 772}$, $b_i \in \mathbb{R}^{768}$ aims to map the relative pose information into the original 768 CLIP features (which is why initially the layer outputs the CLIP embedding with no regards to the camera pose). The other layer $W \in \mathbb{R}^{C \times 768}$, $b \in \mathbb{R}^C$, initialized normally, serves as an interface between the semantic embedding and the transformer architecture by mapping it onto a token. The (W_i, b_i) layer is set to have 10 times the learning rate of other parameters, as in our experiments without this setting the gradient quickly explodes.

3.4. Multi-Scale Local Conditioning

The global encoding is a good condition for generation because it aggregates semantic information across the entire image and has full field-of-view. However, in this process, the details of the original image are lost. Hence we need to add another source of conditioning which can directly provide the autoregressive model with portions of the input image. To this end we propose a local conditioning mechanism which exploits our multi-scale tokenizer to provide effective conditioning information for the attention layers.

As previously shown in Fig. 2, we encode the conditioning image x through the multi-scale VQVAE into tokens the same way as we encode the ground-truth x^* . This ensures that the conditioning tokens and tokens used during generation share the same vocabulary (from the VQVAE codebook Z), thus facilitating the application of self-attention in the next-scale transformer. We extend the block triangular mask such that all conditioning tokens can affect the next attention block’s conditioning and the input tokens, but are not affected by input tokens (as displayed in Fig. 4). This method of conditioning via token prepending is well-suited to the autoregressive nature of our paradigm, and does not require any architectural accommodations. We observe in our ablation studies that this greatly enhances the effectiveness of our method compared to purely using a global encoding as conditioning. We add classifier-free guidance by randomly replacing local conditioning tokens with a learnable null token.

In conventional diffusion-based methods, the predominant way of adding local conditioning is to channel-concatenate the conditioning image onto the latent noise

Table 1. **Quantitative benchmarking results.** We compare against state-of-the-art baselines using diffusion backbones on six well-established benchmarking datasets.

	GSO			ABO			OO3D			Time (s)
	PSNR (\uparrow)	SSIM (\uparrow)	LPIPS (\downarrow)	PSNR (\uparrow)	SSIM (\uparrow)	LPIPS (\downarrow)	PSNR (\uparrow)	SSIM (\uparrow)	LPIPS (\downarrow)	
Zero 1-to-3 [40]	13.39	0.7776	0.2672	12.75	0.7632	0.2901	13.43	0.7737	0.2723	1.84
Zero 123-XL [17]	13.80	0.7865	0.2595	12.78	0.7646	0.2766	14.05	0.7966	0.2516	1.84
EscherNet [35]	16.77	0.8275	0.1891	17.03	0.8381	0.1693	16.12	0.8294	0.2060	1.68
Ours	17.44	0.8491	0.1853	18.82	0.8725	0.1360	18.26	0.8622	0.1617	0.22

	RTMV			NeRF			SNet			Params
	PSNR (\uparrow)	SSIM (\uparrow)	LPIPS (\downarrow)	PSNR (\uparrow)	SSIM (\uparrow)	LPIPS (\downarrow)	PSNR (\uparrow)	SSIM (\uparrow)	LPIPS (\downarrow)	
Zero 1-to-3 [40]	8.49	0.5260	0.4772	10.88	0.6222	0.4146	13.02	0.7957	0.3288	1.0B
Zero 123-XL [17]	8.58	0.5237	0.4735	11.29	0.6551	0.3926	13.29	0.8070	0.3206	1.0B
EscherNet [35]	10.38	0.5327	0.4340	13.85	0.6783	0.2868	16.35	0.8450	0.1951	1.0B
Ours	10.95	0.5739	0.3991	14.51	0.7025	0.2735	19.42	0.8927	0.1300	1.0B

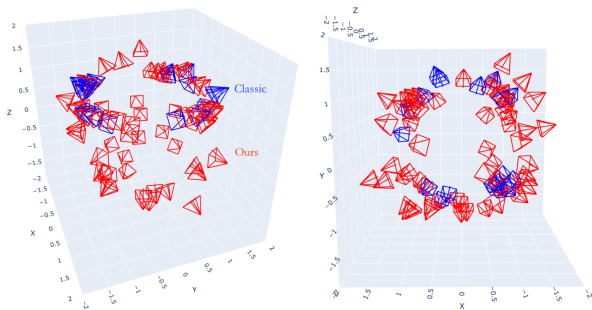


Figure 5. **Improving NVS evaluation.** A free view and a top view of the “classic” input camera views compared to ours (40 each sampled).

used for diffusion. However, as previous works have noted [72], this inherently creates a false pixel-to-pixel correspondence between the conditioning image and the latent whereas the actual relationship is a lot more non-trivial (as transformations in 3D are involved).

Our method, in contrast, does not inherently impose any correspondences. Since the multi-scale encoding is inherently hierarchical, not only can the transformer learn correspondence relationships without any structural assumptions, it can also model more complex relationships that require information from several levels of detail.

4. Experiments

4.1. Training Settings

We use the multi-scale VQVAE checkpoint from [76], which was trained on the OpenImages dataset [37]. We train our models on the Objaverse dataset [18], from which we render 256×256 views with randomly sampled camera poses. The number of 16×16 patches per side for each VQVAE scale follows the progression (1, 2, 3, 4, 5, 6, 8, 10, 13, 16), for a total of 10 prediction steps. The depth of the model is set to be 24 for bench-

marking in order for the model size to be 1.0B, matching diffusion-based baselines. Optimization is conducted via AdamW [42], and implementation uses PyTorch [55]. We trained on 32 NVIDIA H200 GPUs, and tested inference speed on a single H200. We report baseline results from officially recommended default settings.

4.2. Evaluation Settings

We conduct evaluation across six commonly used datasets: Google Scanned Objects (GSO) [20], Amazon Berkeley Objects (ABO) [16], OmniObject3D (OO3D) [87], Ray-Traced Multi-View Synthetic (RTMV) [78], NeRF Synthetic (NeRF) [47], and ShapeNet Core (SNet) [11]. None of those datasets overlap with our training set (Objaverse), which means that all of the experimental results are zero-shot inference.

For all datasets except NeRF, we sample 100 objects randomly, and render 7 views for 3D objects (for RTMV we directly sample 7 views), with one being used as the input view and the other 6 being used for evaluation; for NeRF, we use all 8 objects, sample one random input view from each object’s training set, and evaluate across all 200 testing views.

Improving NVS Benchmarking We notice that benchmarking in previous works have usually inherited the evaluation rendering settings used by Zero 1-to-3 [40]. However, in this “classic” setting, we notice that input views are selected from a narrow range of elevation angles, which makes the task much easier but does not demonstrate the model’s robustness across a wide range of possible views of an object. This is also a discrepancy with the training setting, where camera poses are sampled across an entire viewing sphere (save for very high elevation angles, and with the radial distance varying).

Hence, we choose to make the evaluation setting exactly the same as the training setting. A visual comparison be-

Table 2. **Ablation study results.** We evaluate the necessity of two design choices: adding local conditioning (as in Sec. 3.4), and removing adaptive layer normalization (AdaLN) for the classifier head.

	GSO			ABO			OO3D		
	PSNR (\uparrow)	SSIM (\uparrow)	LPIPS (\downarrow)	PSNR (\uparrow)	SSIM (\uparrow)	LPIPS (\downarrow)	PSNR (\uparrow)	SSIM (\uparrow)	LPIPS (\downarrow)
Global Only	13.25	0.7959	0.2672	13.04	0.7892	0.3116	15.03	0.8161	0.2523
w/ Cls. Head AdaLN	12.76	0.7885	0.2510	12.80	0.7549	0.3131	12.59	0.7832	0.2540
Ours	17.44	0.8491	0.1853	18.82	0.8725	0.1360	18.26	0.8622	0.1617
	RTMV			NeRF			SNet		
	PSNR (\uparrow)	SSIM (\uparrow)	LPIPS (\downarrow)	PSNR (\uparrow)	SSIM (\uparrow)	LPIPS (\downarrow)	PSNR (\uparrow)	SSIM (\uparrow)	LPIPS (\downarrow)
Global Only	8.74	0.4968	0.5124	11.80	0.6280	0.4176	14.52	0.8232	0.2906
w/ Cls. Head AdaLN	7.39	0.4771	0.5301	10.41	0.5958	0.4237	12.73	0.7929	0.2739
Ours	10.95	0.5739	0.3991	14.51	0.7025	0.2735	19.42	0.8927	0.1300

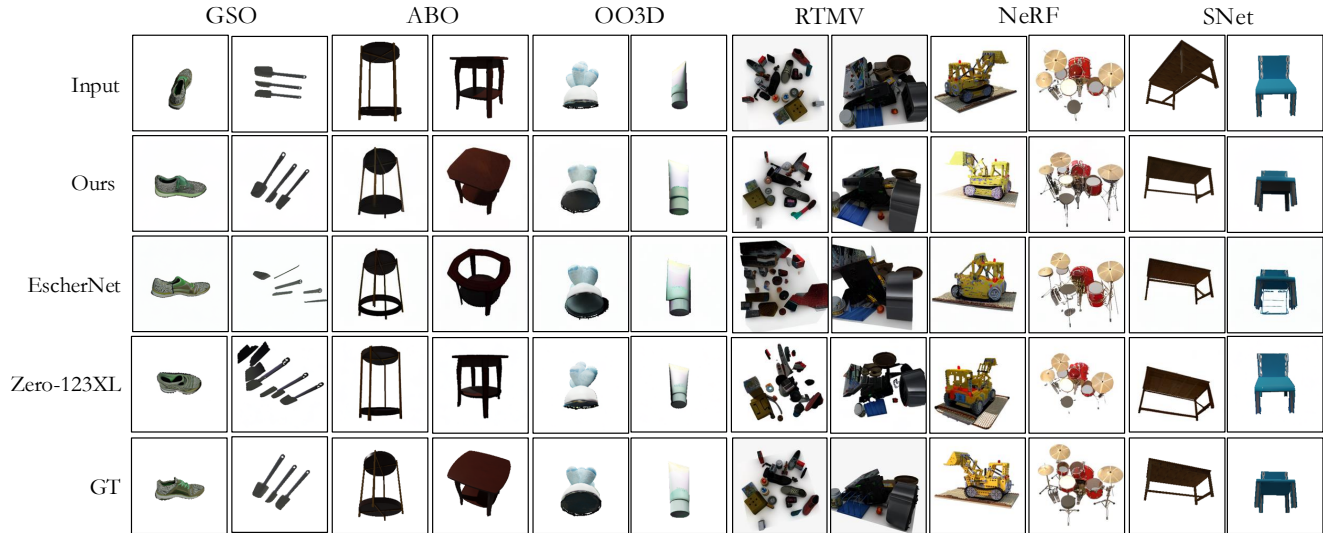


Figure 6. **Qualitative results.** We select a total of 12 cases to visually compare our method with diffusion-based prior works.

tween cameras sampled in our evaluation setting and the “classic” one is in Fig. 5. We note that this makes the task considerably more difficult (but the camera poses are still all within the training range, and hence are not out-of-distribution), and requires models to be more robust with respect to the input pose.

4.3. Results

Benchmarking Quantitative results from our benchmarking are shown in Tab. 1. As shown, our model, while being of the same size as the Stable Diffusion-tuned baselines, is up to more than 8 times faster than those baselines (under their officially recommended settings), and consistently produces significantly better results across our 6 benchmarks.

Qualitative Comparison We present qualitative results in Fig. 6. As shown, our model produces more accurate reconstructions, and also can achieve more realistic and feasible results (e.g., GSO shoe) even though it has seen far

fewer visual information than the diffusion-based baselines (which have gone through 2D pretraining). Furthermore, our model is also good at localizing objects after transformation even in cluttered scenes (e.g., RTMV), and has a good understanding of geometrical structure (e.g., SNet table). Even when outputs are inaccurate due to uncertainty regarding factors such as lighting (e.g., NeRF lego bulldozer), it continues to present accurate geometries and feasible lighting/texture. Surprisingly, although one might expect diffusion-based models would be more capable of predicting unseen portions of objects due to its knowledge of 2D priors, it seems that ours often better (e.g., ABO — note how EscherNet creates counterintuitive holes and Zero-123XL struggles to change viewpoints correctly).

Ablation We compare our model with a version that uses only global encodings, and one that keeps AdaLN with its classifier head. The results in Tab. 2 show that both of the tested design choices were necessary for the model to achieve acceptable results.

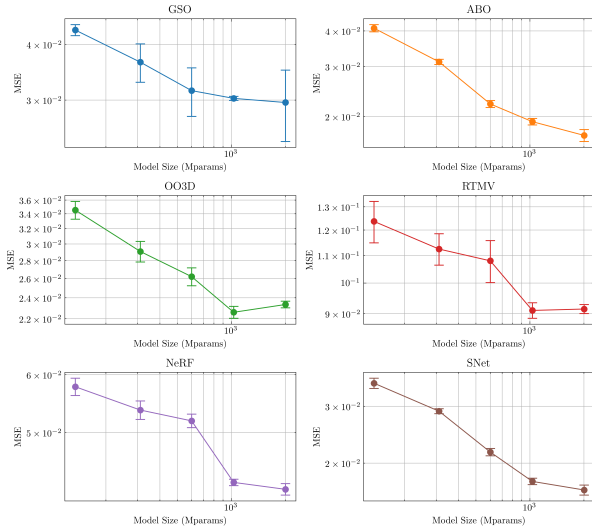


Figure 7. **ArchonView scaling with model size.** The five data points respectively have depth 12, 16, 20, 24, and 30. Error bars are \pm one standard deviation from five repetitions each.

Scaling We investigate the model’s scaling behavior with respect to model size and dataset size (we do not consider scaling with computation due to the difficulty of rigorously defining an optimal stopping point, as in our case performance is not directly tied to token accuracy unlike in other tasks like LLMs). Results are shown in Figs. 7 and 8. It seems that adding more data would likely continue to improve model performance considerably. As for model size, results demonstrate preliminary evidence of scaling law-like behavior below 1B parameters, and the performance of larger models is likely bottlenecked by dataset size.

5. Discussion

5.1. Implications

According to [40], diffusion-based object-centric NVS models work by adapting visual priors inherent in pre-trained 2D diffusion models. This, in turn, causes heavy reliance on large pretrained models such as Stable Diffusion (which was trained on over 2B images [70]). In contrast, we only use the “fine-tuning” dataset of previous works (with 800k 3D objects) and achieved significantly superior results. This demonstrates that under the autoregressive formulation, the 3D objects already contain enough information for the model to accurately, efficiently, and scalably conduct object-centric NVS. Furthermore, trends in Fig. 8 show that increasing the dataset size beyond 800k (Objaverse) is likely to yield further positive results, which gives a clear direction for the next step of scaling ArchonView towards operational usage.

In addition, our superior speed and accuracy suggests the potential for a paradigm shift from diffusion to next-scale

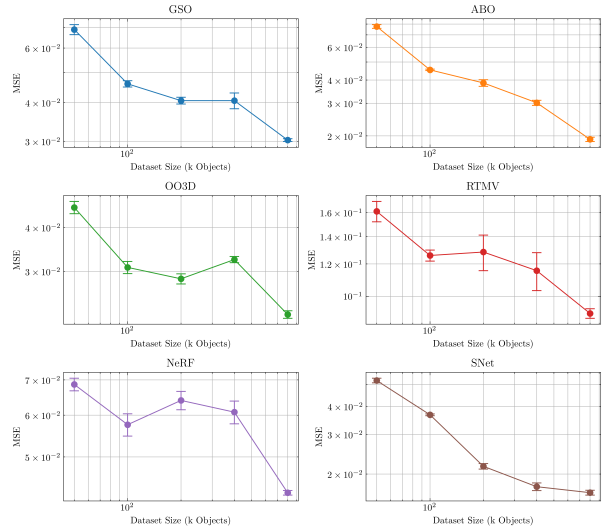


Figure 8. **ArchonView scaling with dataset size.** We randomly subsample objects from our training set and train models with those subsets. Error bars are \pm one standard deviation from five repetitions each.

autoregression in the field of generative NVS, which avoids diffusion’s “original sins” in speed and scalability that stem from the need for repeated denoising steps. Next-scale autoregression is also a rapidly evolving technique, and many advances in this line of research can possibly be used as plug-in improvements to our method. Hence we believe ArchonView can function as a base model for future innovations that can further drive this paradigm shift.

5.2. Potential Negative Social Impacts

Results presented by this work, given their visual generative nature, are prone to being exploited by malicious agents. We encourage responsible usage in accordance with relevant common guidelines. The “Direct Use” portion of the DALL-E Mini model card [52], shared by works such as Stable Diffusion [67], applies well.

6. Conclusion

We introduce the first method of zero-shot single-image object-centric NVS to be based on visual autoregression, using the next-scale autoregression paradigm. We show that it does not require 2D pretraining, achieves state-of-the-art performance across several benchmark tasks, is several times faster in inference time compared to previous methods, and demonstrates scaling behavior with model size and dataset size. This demonstrates the oft-overlooked potential of autoregressive backbones and their advantages over diffusion for NVS tasks, and provides a base model for potential future work in this direction.

Acknowledgments

We would like to thank Xiaoxue Chen (Tsinghua University) and Xin Kong (Imperial College London) for useful discussions.

References

- [1] Jonathan T Barron, Ben Mildenhall, Matthew Tancik, Peter Hedman, Ricardo Martin-Brualla, and Pratul P Srinivasan. Mip-NeRF: A Multiscale Representation for Anti-Aliasing Neural Radiance Fields. In *Proceedings of the IEEE/CVF International Conference on Computer Vision*, pages 5855–5864, 2021. 2
- [2] Jonathan T Barron, Ben Mildenhall, Dor Verbin, Pratul P Srinivasan, and Peter Hedman. Mip-NeRF 360: Unbounded Anti-Aliased Neural Radiance Fields. In *Proceedings of the IEEE/CVF Conference on Computer Vision and Pattern Recognition*, pages 5470–5479, 2022.
- [3] Jonathan T Barron, Ben Mildenhall, Dor Verbin, Pratul P Srinivasan, and Peter Hedman. Zip-NeRF: Anti-Aliased Grid-Based Neural Radiance Fields. In *Proceedings of the IEEE/CVF International Conference on Computer Vision*, pages 19697–19705, 2023. 2
- [4] Miguel Angel Bautista, Pengsheng Guo, Samira Abnar, Walter Talbott, Alexander Toshev, Zhuoyuan Chen, Laurent Dinh, Shuangfei Zhai, Hanlin Goh, Daniel Ulbricht, Afshin Dehghan, and Josh Susskind. GAUDI: A Neural Architect for Immersive 3D Scene Generation. *Advances in Neural Information Processing Systems*, 36:25102–25116, 2022. 3
- [5] Tom B Brown, Benjamin Mann, Nick Ryder, Melanie Subbiah, Jared Kaplan, Prafulla Dhariwal, Arvind Neelakantan, Pranav Shyam, Girish Sastry, Amanda Askell, Sandhini Agarwal, Ariel Herbert-Voss, Gretchen Krueger, Tom Henighan, Rewon Child, Aditya Ramesh, Daniel M Ziegler, Jeffrey Wu, Clemens Winter, Christopher Hesse, Mark Chen, Eric Sigler, Mateusz Litwin, Scott Gray, Benjamin Chess, Jack Clark, Christopher Berner, Sam McCandlish, Alec Radford, Ilya Sutskever, and Dario Amodei. Language Models are Few-Shot Learners. *Advances in Neural Information Processing Systems*, 34, 2020. 2
- [6] Jake Bruce, Michael D Dennis, Ashley Edwards, Jack Parker-Holder, Yuge Shi, Edward Hughes, Matthew Lai, Aditi Mavalankar, Richie Steigerwald, Chris Apps, Yusuf Aytar, Sarah Bechtle, Feryal Behbahani, Stephanie Chan, Nicholas Heess, Lucy Gonzalez, Simon Osindero, Sherjil Ozair, Scott Reed, Jingwei Zhang, Konrad Zolna, Jeff Clune, Nando de Freitas, Satinder Singh, and Tim Rocktäschel. Genie: Generative Interactive Environments. In *International Conference on Machine Learning*, 2024. 2
- [7] Chameleon Team. Chameleon: Mixed-Modal Early-Fusion Foundation Models. *arXiv preprint arXiv:2405.09818*, 2024. 2
- [8] Eric R Chan, Marco Monteiro, Petr Kellnhofer, Jiajun Wu, and Gordon Wetzstein. pi-GAN: Periodic Implicit Generative Adversarial Networks for 3D-Aware Image Synthesis. In *Proceedings of the IEEE/CVF International Conference on Computer Vision*, pages 5799–5809, 2021. 3
- [9] Eric R Chan, Connor Z Lin, Matthew A Chan, Koki Nagano, Boxiao Pan, Shalini De Mello, Orazio Gallo, Leonidas J Guibas, Jonathan Tremblay, Sameh Khamis, Tero Karras, and Gordon Wetzstein. Efficient Geometry-Aware 3D Generative Adversarial Networks. In *Proceedings of the IEEE/CVF Conference on Computer Vision and Pattern Recognition*, pages 16123–16133, 2022. 3
- [10] Eric R Chan, Koki Nagano, Matthew A Chan, Alexander W Bergman, Jeong Joon Park, Axel Levy, Miki Aittala, Shalini De Mello, Tero Karras, and Gordon Wetzstein. Generative Novel View Synthesis with 3D-Aware Diffusion Models. In *Proceedings of the IEEE/CVF International Conference on Computer Vision*, pages 4217–4229, 2023. 3
- [11] Angel X Chang, Thomas Funkhouser, Leonidas Guibas, Pat Hanrahan, Qixing Huang, Zimo Li, Silvio Savarese, Manolis Savva, Shuran Song, Hao Su, Jianxiong Xiao, Li Yi, and Fisher Yu. Shapenet: An Information-Rich 3D Model Repository. *arXiv preprint arXiv:1512.03012*, 2015. 3, 6
- [12] Anpei Chen, Zexiang Xu, Fuqiang Zhao, Xiaoshuai Zhang, Fanbo Xiang, Jingyi Yu, and Hao Su. MVS-NeRF: Fast Generalizable Radiance Field Reconstruction from Multi-View Stereo. In *Proceedings of the IEEE/CVF International Conference on Computer Vision*, pages 14124–14133, 2021. 3
- [13] Anpei Chen, Zexiang Xu, Andreas Geiger, Jingyi Yu, and Hao Su. TensorRF: Tensorial Radiance Fields. In *European Conference on Computer Vision*, pages 333–350. Springer, 2022. 2
- [14] Mark Chen, Alec Radford, Rewon Child, Jeffrey Wu, Heewoo Jun, David Luan, and Ilya Sutskever. Generative Pretraining from Pixels. In *International Conference on Machine Learning*, pages 1691–1703. PMLR, 2020. 2
- [15] Julian Chibane, Aayush Bansal, Verica Lazova, and Gerard Pons-Moll. Stereo Radiance Fields (SRF): Learning View Synthesis for Sparse Views of Novel Scenes. In *Proceedings of the IEEE/CVF Conference on Computer Vision and Pattern Recognition*, pages 7911–7920, 2021. 3

- [16] Jasmine Collins, Shubham Goel, Kenan Deng, Achleshwar Luthra, Leon Xu, Erhan Gundogdu, Xi Zhang, Tomas F Yago Vicente, Thomas Dideriksen, Himanshu Arora, Matthieu Guillaumin, and Jitendra Malik. ABO: Dataset and Benchmarks for Real-World 3D Object Understanding. In *Proceedings of the IEEE/CVF Conference on Computer Vision and Pattern Recognition*, pages 21126–21136, 2022. 6
- [17] Matt Deitke, Ruoshi Liu, Matthew Wallingford, Huong Ngo, Oscar Michel, Aditya Kusupati, Alan Fan, Christian Laforte, Vikram Voleti, Samir Yitzhak Gadre, Eli Vanderbilt, Kiana Ehsani, Ludwig Schmidt, and Ali Farhadi. Objaverse-XL: A Universe of 10M+ 3D Objects. *Advances in Neural Information Processing Systems*, 37:35799–35813, 2023. 6
- [18] Matt Deitke, Dustin Schwenk, Jordi Salvador, Luca Weihs, Oscar Michel, Eli Vanderbilt, Ludwig Schmidt, Kiana Ehsani, Aniruddha Kembhavi, and Ali Farhadi. Objaverse: A Universe of Annotated 3D Objects. In *Proceedings of the IEEE/CVF Conference on Computer Vision and Pattern Recognition*, pages 13142–13153, 2023. 6
- [19] Congyue Deng, Chiyu Jiang, Charles R Qi, Xinchen Yan, Yin Zhou, Leonidas Guibas, and Dragomir Anguelov. NeRDi: Single-View NeRF Synthesis with Language-Guided Diffusion as General Image Priors. In *Proceedings of the IEEE/CVF Conference on Computer Vision and Pattern Recognition*, pages 20637–20647, 2023. 3
- [20] Laura Downs, Anthony Francis, Nate Koenig, Brandon Kinman, Ryan Hickman, Krista Reymann, Thomas B McHugh, and Vincent Vanhoucke. Google Scanned Objects: A High-Quality Dataset of 3D Scanned Household Items. In *International Conference on Robotics and Automation*, pages 2553–2560. IEEE, 2022. 6
- [21] Patrick Esser, Robin Rombach, and Bjorn Ommer. Taming Transformers for High-Resolution Image Synthesis. In *Proceedings of the IEEE/CVF Conference on Computer Vision and Pattern Recognition*, pages 12873–12883, 2021. 2
- [22] Sara Fridovich-Keil, Alex Yu, Matthew Tancik, Qin-hong Chen, Benjamin Recht, and Angjoo Kanazawa. Plenoxels: Radiance Fields without Neural Networks. In *Proceedings of the IEEE/CVF Conference on Computer Vision and Pattern Recognition*, pages 5501–5510, 2022. 2
- [23] Matheus Gadelha, Subhransu Maji, and Rui Wang. 3D Shape Induction from 2D Views of Multiple Objects. In *International Conference on 3D Vision*, pages 402–411. IEEE, 2017. 3
- [24] Ian Goodfellow, Jean Pouget-Abadie, Mehdi Mirza, Bing Xu, David Warde-Farley, Sherjil Ozair, Aaron Courville, and Yoshua Bengio. Generative Adversarial Nets. *Advances in Neural Information Processing Systems*, 28, 2014. 3
- [25] Jiatao Gu, Yuyang Wang, Yizhe Zhang, Qihang Zhang, Dinghui Zhang, Navdeep Jaitly, Josh Susskind, and Shuangfei Zhai. DART: Denoising Autoregressive Transformer for Scalable Text-to-Image Generation. *arXiv preprint arXiv:2410.08159*, 2024. 2
- [26] Jian Han, Jinlai Liu, Yi Jiang, Bin Yan, Yuqi Zhang, Zehuan Yuan, Bingyue Peng, and Xiaobing Liu. Infinity: Scaling Bitwise Autoregressive Modeling for High-Resolution Image Synthesis. *arXiv preprint arXiv:2412.04431*, 2024. 2
- [27] Tom Henighan, Jared Kaplan, Mor Katz, Mark Chen, Christopher Hesse, Jacob Jackson, Heewoo Jun, Tom B Brown, Prafulla Dhariwal, Scott Gray, Chris Hallacy, Benjamin Mann, Alec Radford, Aditya Ramesh, Nick Ryder, Daniel M Ziegler, John Schulman, Dario Amodei, and Sam McCandlish. Scaling Laws for Autoregressive Generative Modeling. *arXiv preprint arXiv:2010.14701*, 2020. 2
- [28] Jonathan Ho and Tim Salimans. Classifier-Free Diffusion Guidance. *NeurIPS Workshop on Deep Generative Models and Downstream Applications*, 2021. 2
- [29] Binbin Huang, Zehao Yu, Anpei Chen, Andreas Geiger, and Shenghua Gao. 2D Gaussian Splatting for Geometrically Accurate Radiance Fields. In *ACM SIGGRAPH*, pages 1–11, 2024. 2
- [30] Ajay Jain, Matthew Tancik, and Pieter Abbeel. Putting NeRF on a Diet: Semantically Consistent Few-Shot View Synthesis. In *Proceedings of the IEEE/CVF International Conference on Computer Vision*, pages 5885–5894, 2021. 3
- [31] Jared Kaplan, Sam McCandlish, Tom Henighan, Tom B Brown, Benjamin Chess, Rewon Child, Scott Gray, Alec Radford, Jeffrey Wu, and Dario Amodei. Scaling Laws for Neural Language Models. *arXiv preprint arXiv:2001.08361*, 2020. 2
- [32] Chris Kelly, Luhui Hu, Bang Yang, Yu Tian, Deshun Yang, Cindy Yang, Zaoshan Huang, Zihao Li, Jiayin Hu, and Yuexian Zou. VisionGPT: Vision-Language Understanding Agent Using Generalized Multimodal Framework. *arXiv preprint arXiv:2403.09027*, 2024. 2
- [33] Bernhard Kerbl, Georgios Kopanas, Thomas Leimkühler, and George Drettakis. 3D Gaussian Splatting for Real-Time Radiance Field Rendering. *ACM Transactions on Graphics*, 42(4):139–1, 2023. 2
- [34] Dan Kondratyuk, Lijun Yu, Xiuye Gu, José Lezama, Jonathan Huang, Grant Schindler, Rachel Hornung,

- Vighnesh Birodkar, Jimmy Yan, Ming-Chang Chiu, Krishna Somandepalli, Hassan Akbari, Yair Alon, Yong Cheng, Josh Dillon, Agrim Gupta, Meera Hahn, Anja Hauth, David Hendon, Alonso Martinex, David Minnen, Mikhail Sirotenko, Kihyuk Sohn, Xuan Yang, Hartwig Adam, Ming-Hsuan Yang, Irfan Essa, Huisheng Wang, David A Ross, and Bryan Seybold. Videopoet: A Large Language Model for Zero-Shot Video Generation. In *International Conference on Machine Learning*. PMLR, 2024. 2
- [35] Xin Kong, Shikun Liu, Xiaoyang Lyu, Marwan Taher, Xiaojuan Qi, and Andrew J Davison. EscherNet: A Generative Model for Scalable View Synthesis. In *Proceedings of the IEEE/CVF Conference on Computer Vision and Pattern Recognition*, pages 9503–9513, 2024. 3, 6
- [36] Jonáš Kulhánek, Erik Derner, Torsten Sattler, and Robert Babuška. Viewformer: Nerf-Free Neural Rendering from Few Images using Transformers. In *European Conference on Computer Vision*, pages 198–216. Springer, 2022. 3
- [37] Alina Kuznetsova, Hassan Rom, Neil Alldrin, Jasper Uijlings, Ivan Krasin, Jordi Pont-Tuset, Shahab Kamali, Stefan Popov, Matteo Mallocci, Alexander Kolesnikov, Tom Duerig, and Vittorio Ferrari. The Open Images Dataset v4: Unified Image Classification, Object Detection, and Visual Relationship Detection at Scale. *International Journal of Computer Vision*, 128(7):1956–1981, 2020. 6
- [38] Doyup Lee, Chiheon Kim, Saehoon Kim, Minsu Cho, and Wook-Shin Han. Autoregressive Image Generation Using Residual Quantization. In *Proceedings of the IEEE/CVF Conference on Computer Vision and Pattern Recognition*, pages 11523–11532, 2022. 2
- [39] Zongming Li, Tianheng Cheng, Shoufa Chen, Peize Sun, Haocheng Shen, Longjin Ran, Xiaoxin Chen, Wenyu Liu, and Xinggang Wang. ControlAR: Controllable Image Generation with Autoregressive Models. *arXiv preprint arXiv:2410.02705*, 2024. 2
- [40] Ruoshi Liu, Rundi Wu, Basile Van Hoorick, Pavel Tokmakov, Sergey Zakharov, and Carl Vondrick. Zero-1-to-3: Zero-Shot One Image to 3D Object. In *Proceedings of the IEEE/CVF International Conference on Computer Vision*, pages 9298–9309, 2023. 3, 5, 6, 8
- [41] Yuan Liu, Cheng Lin, Zijiao Zeng, Xiaoxiao Long, Lingjie Liu, Taku Komura, and Wenping Wang. SyncDreamer: Generating Multiview-Consistent Images from a Single-View Image. In *International Conference on Learning Representations*, 2024. 3
- [42] Ilya Loshchilov and Frank Hutter. Decoupled Weight Decay Regularization. In *International Conference on Learning Representations*, 2019. 6
- [43] Taiming Lu, Tianmin Shu, Junfei Xiao, Luoxin Ye, Jiahao Wang, Cheng Peng, Chen Wei, Daniel Khashabi, Rama Chellappa, Alan Yuille, and Jieneng Chen. GenEx: Generating an Explorable World. *arXiv preprint arXiv:2412.09624*, 2024. 2
- [44] Xiaoxiao Ma, Mohan Zhou, Tao Liang, Yalong Bai, Tiejun Zhao, Huaian Chen, and Yi Jin. STAR: Scale-Wise Text-to-Image Generation via Auto-Regressive Representations. *arXiv preprint arXiv:2406.10797*, 2024. 2
- [45] Alexander Mai, Peter Hedman, George Kopanas, Dor Verbin, David Futschik, Qiangeng Xu, Falko Kuester, Jonathan T Barron, and Yinda Zhang. EVER: Exact Volumetric Ellipsoid Rendering for Real-Time View Synthesis. *arXiv preprint arXiv:2410.01804*, 2024. 2
- [46] Luke Melas-Kyriazi, Iro Laina, Christian Ruppert, and Andrea Vedaldi. RealFusion: 360° Reconstruction of Any Object from a Single Image. In *Proceedings of the IEEE/CVF Conference on Computer Vision and Pattern Recognition*, pages 8446–8455, 2023. 3
- [47] Ben Mildenhall, Pratul P Srinivasan, Matthew Tan-cik, Jonathan T Barron, Ravi Ramamoorthi, and Ren Ng. NeRF: Representing Scenes as Neural Radiance Fields for View Synthesis. *Communications of the ACM*, 65(1):99–106, 2021. 2, 6
- [48] Thomas Müller, Alex Evans, Christoph Schied, and Alexander Keller. Instant Neural Graphics Primitives with a Multiresolution Hash Encoding. *ACM Transactions on Graphics*, 41(4):1–15, 2022. 2
- [49] Thu Nguyen-Phuoc, Chuan Li, Lucas Theis, Christian Richardt, and Yong-Liang Yang. HoloGAN: Unsupervised Learning of 3D Representations from Natural Images. In *Proceedings of the IEEE/CVF International Conference on Computer Vision*, pages 7588–7597, 2019. 3
- [50] Michael Niemeyer and Andreas Geiger. GIRAFFE: Representing Scenes as Compositional Generative Neural Feature Fields. In *Proceedings of the IEEE/CVF Conference on Computer Vision and Pattern Recognition*, pages 11453–11464, 2021. 3
- [51] Michael Niemeyer, Jonathan T Barron, Ben Mildenhall, Mehdi SM Sajjadi, Andreas Geiger, and Noha Radwan. RegNeRF: Regularizing Neural Radiance Fields for View Synthesis from Sparse Inputs. In *Proceedings of the IEEE/CVF Conference on Computer Vision and Pattern Recognition*, pages 5480–5490, 2022. 3
- [52] OpenAI. DALL-E Mini Model Card, 2022. <https://huggingface.co/dalle-mini/dalle-mini>. 8
- [53] OpenAI. GPT-4V(ision) System Card, 2023. <https://openai.com/index/gpt-4v-system-card>. 2

- [54] Niki Parmar, Ashish Vaswani, Jakob Uszkoreit, Lukasz Kaiser, Noam Shazeer, Alexander Ku, and Dustin Tran. Image Transformer. In *International Conference on Machine Learning*, pages 4055–4064. PMLR, 2018. 2
- [55] Adam Paszke, Sam Gross, Francisco Massa, Adam Lerer, James Bradbury, Gregory Chanan, Trevor Killeen, Zeming Lin, Natalia Gimelshein, Luca Antiga, Alban Desmaison, Andreas Köpf, Edward Yang, Zach DeVito, Martin Raison, Alykhan Tejani, Sasank Chilamkurthy, Benoit Steiner, Lu Fang, Junjie Bai, and Soumith Chintala. PyTorch: An Imperative Style, High-Performance Deep Learning Library. *Advances in Neural Information Processing Systems*, 33, 2019. 6
- [56] William Peebles and Saining Xie. Scalable Diffusion Models with Transformers. In *Proceedings of the IEEE/CVF International Conference on Computer Vision*, pages 4195–4205, 2023. 2, 5
- [57] Justin Pinkney. Stable Diffusion Image Variations, 2023. <https://www.justinpinkney.com/blog/2023/stable-diffusion-image-variations>. 3
- [58] Reiner Pope, Sholto Douglas, Aakanksha Chowdhery, Jacob Devlin, James Bradbury, Jonathan Heek, Ke-fan Xiao, Shivani Agrawal, and Jeff Dean. Efficiently Scaling Transformer Inference. *Proceedings of Machine Learning and Systems*, 5:606–624, 2023. 5
- [59] Alec Radford, Karthik Narasimhan, Tim Salimans, and Ilya Sutskever. Improving Language Understanding by Generative Pre-Training, 2018. <https://openai.com/index/language-unsupervised>. 2
- [60] Alec Radford, Jeffrey Wu, Rewon Child, David Luan, Dario Amodei, and Ilya Sutskever. Language Models are Unsupervised Multitask Learners. *OpenAI Blog*, 1 (8):9, 2019. 2
- [61] Alec Radford, Jong Wook Kim, Chris Hallacy, Aditya Ramesh, Gabriel Goh, Sandhini Agarwal, Girish Sastry, Amanda Askell, Pamela Mishkin, Jack Clark, Gretchen Krueger, and Ilya Sutskever. Learning Transferable Visual Models from Natural Language Supervision. In *International Conference on Machine Learning*, pages 8748–8763. PMLR, 2021. 5
- [62] Aditya Ramesh, Mikhail Pavlov, Gabriel Goh, Scott Gray, Chelsea Voss, Alec Radford, Mark Chen, and Ilya Sutskever. Zero-Shot Text-to-Image Generation. In *International Conference on Machine Learning*, pages 8821–8831. PMLR, 2021. 2
- [63] Ali Razavi, Aaron Van den Oord, and Oriol Vinyals. Generating Diverse High-Fidelity Images with VQ-VAE-2. *Advances in Neural Information Processing Systems*, 33, 2019. 2
- [64] Sucheng Ren, Qihang Yu, Ju He, Xiaohui Shen, Alan Yuille, and Liang-Chieh Chen. FlowAR: Scale-Wise Autoregressive Image Generation Meets Flow Matching. *arXiv preprint arXiv:2412.15205*, 2024. 2
- [65] Sucheng Ren, Yaodong Yu, Nataniel Ruiz, Feng Wang, Alan Yuille, and Cihang Xie. M-VAR: Decoupled Scale-wise Autoregressive Modeling for High-Quality Image Generation. *arXiv preprint arXiv:2411.10433*, 2024. 2
- [66] Robin Rombach, Patrick Esser, and Björn Ommer. Geometry-Free View Synthesis: Transformers and no 3D Priors. In *Proceedings of the IEEE/CVF International Conference on Computer Vision*, pages 14356–14366, 2021. 3
- [67] Robin Rombach, Andreas Blattmann, Dominik Lorenz, Patrick Esser, and Björn Ommer. High-Resolution Image Synthesis with Latent Diffusion Models. In *Proceedings of the IEEE/CVF Conference on Computer Vision and Pattern Recognition*, pages 10684–10695, 2022. 2, 3, 8
- [68] Mehdi SM Sajjadi, Henning Meyer, Etienne Pot, Urs Bergmann, Klaus Greff, Noha Radwan, Suhani Vora, Mario Lučić, Daniel Duckworth, Alexey Dosovitskiy, Jakob Uszkoreit, Thomas Funkhouser, and Andrea Tagliasacchi. Scene Representation Transformer: Geometry-Free Novel View Synthesis through Set-Latent Scene Representations. In *Proceedings of the IEEE/CVF Conference on Computer Vision and Pattern Recognition*, pages 6229–6238, 2022. 3
- [69] Kyle Sargent, Zizhang Li, Tanmay Shah, Charles Herrmann, Hong-Xing Yu, Yunzhi Zhang, Eric Ryan Chan, Dmitry Lagun, Li Fei-Fei, Deqing Sun, and Jiajun Wu. ZeroNVS: Zero-Shot 360-Degree View Synthesis from a Single Real Image. In *Proceedings of the IEEE/CVF Conference on Computer Vision and Pattern Recognition*, pages 9420–9429, 2024. 3
- [70] Christoph Schuhmann, Romain Beaumont, Richard Vencu, Cade Gordon, Ross Wightman, Mehdi Cherti, Theo Coombes, Aarush Katta, Clayton Mullis, Mitchell Wortsman, Patrick Schramowski, Srivatsa Kundurthy, Katherine Crowson, Ludwig Schmidt, Robert Kaczmarczyk, and Jenia Jitsev. LAION-5B: An Open Large-Scale Dataset for Training Next Generation Image-Text Models. *Advances in Neural Information Processing Systems*, 36:25278–25294, 2022. 8
- [71] Katja Schwarz, Axel Sauer, Michael Niemeyer, Yiyi Liao, and Andreas Geiger. VoxGRAF: Fast 3D-Aware Image Synthesis with Sparse Voxel Grids. *Advances in Neural Information Processing Systems*, 36:33999–34011, 2022. 3
- [72] Ruoxi Shi, Hansheng Chen, Zhuoyang Zhang, Minghua Liu, Chao Xu, Xinyue Wei, Linghao Chen, Chong Zeng, and Hao Su. Zero123++: A Single Im-

- age to Consistent Multi-View Diffusion Base Model. *arXiv preprint arXiv:2310.15110*, 2023. 3, 6
- [73] Cheng Sun, Min Sun, and Hwann-Tzong Chen. Direct Voxel Grid Optimization: Super-Fast Convergence for Radiance Fields Reconstruction. In *Proceedings of the IEEE/CVF Conference on Computer Vision and Pattern Recognition*, pages 5459–5469, 2022. 2
- [74] Quan Sun, Qiyang Yu, Yufeng Cui, Fan Zhang, Xiaosong Zhang, Yueze Wang, Hongcheng Gao, Jingjing Liu, Tiejun Huang, and Xinlong Wang. Emu: Generative Pretraining in Multimodality. In *International Conference on Learning Representations*, 2023. 2
- [75] Haotian Tang, Yecheng Wu, Shang Yang, Enze Xie, Junsong Chen, Junyu Chen, Zhuoyang Zhang, Han Cai, Yao Lu, and Song Han. HART: Efficient Visual Generation with Hybrid Autoregressive Transformer. In *International Conference on Learning Representations*, 2025. 2
- [76] Keyu Tian, Yi Jiang, Zehuan Yuan, Bingyue Peng, and Liwei Wang. Visual Autoregressive Modeling: Scalable Image Generation via Next-Scale Prediction. *Advances in Neural Information Processing Systems*, 38, 2024. 2, 4, 5, 6
- [77] Hugo Touvron, Thibaut Lavril, Gautier Izacard, Xavier Martinet, Marie-Anne Lachaux, Timothée Lacroix, Baptiste Rozière, Naman Goyal, Eric Hambro, Faisal Azhar, et al. Llama: Open and Efficient Foundation Language Models. *arXiv preprint arXiv:2302.13971*, 2023. 2
- [78] Jonathan Tremblay, Moustafa Meshry, Alex Evans, Jan Kautz, Alexander Keller, Sameh Khamis, Thomas Müller, Charles Loop, Nathan Morrical, Koki Nagano, et al. Rtmv: A ray-traced multi-view synthetic dataset for novel view synthesis. *arXiv preprint arXiv:2205.07058*, 2022. 6
- [79] Yuanpeng Tu, Hao Luo, Xi Chen, Sihui Ji, Xiang Bai, and Hengshuang Zhao. VideoAnydoor: High-Fidelity Video Object Insertion with Precise Motion Control. *arXiv preprint arXiv:2501.01427*, 2025. 2
- [80] Aaron Van Den Oord, Oriol Vinyals, and Koray Kavukcuoglu. Neural Discrete Representation Learning. *Advances in Neural Information Processing Systems*, 31, 2017. 2, 4
- [81] Ashish Vaswani, Noam Shazeer, Niki Parmar, Jakob Uszkoreit, Llion Jones, Aidan Gomez, Lukasz Kaiser, and Illia Polosukhin. Attention is All You Need. *Advances in Neural Information Processing Systems*, 31, 2017. 5
- [82] Guangcong Wang, Zhaoxi Chen, Chen Change Loy, and Ziwei Liu. SparseNeRF: Distilling Depth Ranking for Few-Shot Novel View Synthesis. In *Proceedings of the IEEE/CVF International Conference on Computer Vision*, pages 9065–9076, 2023. 3
- [83] Daniel Watson, William Chan, Ricardo Martin-Brualla, Jonathan Ho, Andrea Tagliasacchi, and Mohammad Norouzi. Novel View Synthesis with Diffusion Models. In *International Conference on Learning Representations*, 2023. 3
- [84] Daniel Watson, William Chan, Ricardo Martin-Brualla, Jonathan Ho, Andrea Tagliasacchi, and Mohammad Norouzi. Consistent123: Improve Consistency for One Image to 3D Object Synthesis. In *International Conference on Learning Representations*, 2024. 3
- [85] Chenfei Wu, Jian Liang, Lei Ji, Fan Yang, Yuejian Fang, Daxin Jiang, and Nan Duan. NÜWA: Visual Synthesis Pre-training for Neural Visual World Creation. In *European Conference on Computer Vision*, pages 720–736. Springer, 2022. 2
- [86] Rundi Wu, Ben Mildenhall, Philipp Henzler, Keunhong Park, Ruiqi Gao, Daniel Watson, Pratul P Srinivasan, Dor Verbin, Jonathan T Barron, Ben Poole, and Aleksander Holyński. ReconFusion: 3D Reconstruction with Diffusion Priors. In *Proceedings of the IEEE/CVF Conference on Computer Vision and Pattern Recognition*, pages 21551–21561, 2024. 3
- [87] Tong Wu, Jiarui Zhang, Xiao Fu, Yuxin Wang, Jiawei Ren, Liang Pan, Wayne Wu, Lei Yang, Jiaqi Wang, Chen Qian, Dahua Lin, and Ziwei Liu. Omniobject3d: Large-vocabulary 3d object dataset for realistic perception, reconstruction and generation. In *Proceedings of the IEEE/CVF Conference on Computer Vision and Pattern Recognition*, pages 803–814, 2023. 6
- [88] Dejia Xu, Yifan Jiang, Peihao Wang, Zhiwen Fan, Humphrey Shi, and Zhangyang Wang. SinNeRF: Training Neural Radiance Fields on Complex Scenes from a Single Image. In *European Conference on Computer Vision*, pages 736–753. Springer, 2022. 3
- [89] Wilson Yan, Yunzhi Zhang, Pieter Abbeel, and Aravind Srinivas. VideoGPT: Video Generation Using VQ-VAE and Transformers. *arXiv preprint arXiv:2104.10157*, 2021. 2
- [90] Ziyu Yao, Jialin Li, Yifeng Zhou, Yong Liu, Xi Jiang, Chengjie Wang, Feng Zheng, Yuexian Zou, and Lei Li. CAR: Controllable Autoregressive Modeling for Visual Generation. *arXiv preprint arXiv:2410.04671*, 2024. 2
- [91] Jianglong Ye, Peng Wang, Kejie Li, Yichun Shi, and Heng Wang. Consistent-1-to-3: Consistent Image to 3D View Synthesis via Geometry-Aware Diffusion Models. In *International Conference on 3D Vision*, pages 664–674. IEEE, 2024. 3
- [92] Alex Yu, Ruilong Li, Matthew Tancik, Hao Li, Ren Ng, and Angjoo Kanazawa. Plenotrees for Real-Time

- Rendering of Neural Radiance Fields. In *Proceedings of the IEEE/CVF International Conference on Computer Vision*, pages 5752–5761, 2021. [2](#)
- [93] Alex Yu, Vickie Ye, Matthew Tancik, and Angjoo Kanazawa. PixelNeRF: Neural Radiance Fields from One or Few Images. In *Proceedings of the IEEE/CVF Conference on Computer Vision and Pattern Recognition*, pages 4578–4587, 2021. [3](#)
- [94] Jiahui Yu, Xin Li, Jing Yu Koh, Han Zhang, Ruoming Pang, James Qin, Alexander Ku, Yuanzhong Xu, Jason Baldridge, and Yonghui Wu. Vector-Quantized Image Modeling with Improved VQGAN. In *International Conference on Learning Representations*, 2022. [2](#)
- [95] Jiahui Yu, Yuanzhong Xu, Jing Yu Koh, Thang Luong, Gunjan Baid, Zirui Wang, Vijay Vasudevan, Alexander Ku, Yinfei Yang, Burcu Karagol Ayan, Ben Hutchinson, Wei Han, Zarana Parekh, Xin Li, Han Zhang, Jason Baldridge, and Yonghui Wu. Scaling Autoregressive Models for Content-Rich Text-to-Image Generation. *Transactions on Machine Learning Research*, 2022. [2](#)
- [96] Lvmin Zhang, Anyi Rao, and Maneesh Agrawala. Adding Conditional Control to Text-to-Image Diffusion Models. In *Proceedings of the IEEE/CVF International Conference on Computer Vision*, pages 3836–3847, 2023. [2](#)
- [97] Qian Zhang, Xiangzi Dai, Ninghua Yang, Xiang An, Ziyong Feng, and Xingyu Ren. VAR-CLIP: Text-to-Image Generator with Visual Auto-Regressive Modeling. *arXiv preprint arXiv:2408.01181*, 2024. [2](#)
- [98] Chuanxia Zheng and Andrea Vedaldi. Free3D: Consistent Novel View Synthesis without 3D Representation. In *Proceedings of the IEEE/CVF Conference on Computer Vision and Pattern Recognition*, pages 9720–9731, 2024. [3](#)